

# Microfluidic synthesis of copper nanofluids

Yuxiang Zhang · Wei Jiang · Liqiu Wang

Received: 17 November 2009 / Accepted: 11 February 2010 / Published online: 19 March 2010  
© Springer-Verlag 2010

**Abstract** Copper nanofluids have been chemically synthesized by using home-made microfluidic reactors and by using a boiling flask-3-neck. The influence of flow rates of reactants, reactants concentrations, and surfactant concentrations on copper particle size and size distribution has been investigated. It has been found that neither of them has much influence on particle size and size distribution of copper nanoparticles synthesized in microfluidic reactors due to the fast and efficient mass diffusion in microscale dimension. The copper nanoparticles have an average size of about 3.4 nm with a relatively narrow size distribution of around 22% evaluated by the coefficient of variation. While the average size of copper nanoparticles synthesized by flask method changes from 2.7 to 4.9 nm with a coefficient of variation larger than 30%, depending on concentrations of  $[\text{Cu}(\text{NH}_3)_4] \cdot (\text{OH})_2$  and surfactant sodium dodecylbenzenesulfonate. In addition, by using microfluidic reactors the synthesis time of copper nanofluids can be reduced as much as one order of magnitude, from ~10 min to ~28 s.

**Keywords** Microfluidic reactor · Chemical synthesis · Copper nanofluids · Copper nanoparticles

## 1 Introduction

Nanofluids are stably dilute suspensions of nanomaterials including nanoparticles, nanotubes, and nanofibers. After first proposed by Choi, nanofluids have attracted intensive

energy from thermal society due to their excellent performance in heat transfer (Choi 1995; Das et al. 2006; Trisaksri and Wongwises 2007; Wang and Wei 2009; Wen et al. 2009). In clinical studies, magnetic nanofluids have been successfully applied to treat patients with cancers (Cashion et al. 1999; Chen and Liao 2002). Two methods have been proposed to produce nanofluids: the two-step method and the one-step method. In the two-step method nanoparticles are first fabricated out and then redispersed in based fluids (Lee et al. 1999; Xuan and Li 2000; Wang and Mujumdar 2008). In this method the aggregation of nanoparticles resulted from separation process usually cause poor stability of nanofluids after redispersion. In one-step method nanoparticles are fabricated out in based fluids directly, no redispersion process needed, by either vacuum evaporation onto a running oil substrate (VEROS) (Yatsuya et al. 1978; Yatsuya et al. 1984), or submerged arc nanoparticle synthesis system (SANSS) (Chang et al. 2004; Lo et al. 2005a, b), or chemical synthesis in flasks (Zhu et al. 2004; Liu et al. 2006; Wei et al. 2009). Nanoparticle size produced by the methods mentioned above is normally hard to be controlled and the size distribution is relatively broad. More recently, microfluidic method as a promising technology has been reported superior to traditional methods for producing high quality nanoparticles due to the advantage of eliminating local variations in reaction conditions such as concentration and temperature and of allowing rapid, reproducible change in these conditions. Many kinds of nanoparticles have been synthesized in microfluidic reactors by either continuous stream reaction or segmented gas/liquid flow, which involves semiconductor quantum dots (Jackman et al. 2001; Edel et al. 2002; Chan et al. 2003; Krishnadasan et al. 2004; Shestopalov et al. 2004; Chan et al. 2005), metallic nanoparticles (Wang et al. 2002; Wagner et al. 2003; Song et al. 2004,

Y. Zhang · W. Jiang · L. Wang (✉)  
Department of Mechanical Engineering, The University  
of Hong Kong, Pokfulam Road, Hong Kong, China  
e-mail: lqwang@hku.hk

2005, 2006; Xue et al. 2004; Wagner and Kohler 2005; Shalom et al. 2007), composite nanoparticles (Wang et al. 2004; Kohler et al. 2008), and polymeric nanoparticles (Karnik et al. 2008; Laulicht et al. 2008). However, a systematic investigation on the influence of involving parameters, like flow rates of reactants, reactants concentrations, and surfactant concentrations, is still limited. In this work, we synthesize copper nanofluids by directly mixing the reactants in microfluidic reactors. The influence of flow rates of reactants, reactants concentrations, and surfactant concentrations on copper particle size and size distribution is investigated as well as the stability of copper nanofluids.

## 2 Experiment

### 2.1 Chemicals and materials

Hydrazine hydrate (98%) and copper hydroxide (99.9%) were purchased from Sigma Aldrich Inc. (USA). Sodium dodecylbenzenesulfonate (DBS), chloride acid, and trisodium phosphate (Tris) were purchased from Tianjin Damao Chemical Reagent Co., Ltd. (China). Ammonia solution (25%) was bought from Tianjin Fuyu Fine Chemical Industry Co., Ltd. (China). Deionized (DI) water was prepared by an in-house ion exchange system with ultrasonic treatment before use to dispel the dissolved air. All reagents were of reagent grade and used as received without further purification.

### 2.2 Stock solutions preparation

A typical synthesis procedure involved the preparation of two stock solutions: the first was a dilute  $[\text{Cu}(\text{NH}_3)_4](\text{OH})_2$  solution, and the second was a dilute hydrazine hydrate solution containing stabilizer DBS. Stock solution  $[\text{Cu}(\text{NH}_3)_4](\text{OH})_2$  was freshly prepared by dissolving 0.195 g copper hydroxide into 40 ml dense ammonia solution (25%) followed by being diluted to 100 ml with diluted ammonia solution (1 M), resulting in a concentration of 20 mM. Different concentrations of  $[\text{Cu}(\text{NH}_3)_4](\text{OH})_2$  solution used in the experiment, from 0.5 to 8 mM, were obtained by diluting corresponding amount of stock solution with DI water to 20 ml. The reducing solutions were prepared by dissolving corresponding amount of hydrazine hydrate in 20 ml DI water such that the molar concentration ratio of hydrazine to copper complex  $[\text{Cu}(\text{NH}_3)_4](\text{OH})_2$  was always kept at 30:1. Different amount of DBS was added into the reducing solution before synthesizing in order to stabilize the resulted nanofluids. A buffer solution, pH = 8.5, was prepared by mixing 50 ml Tris solution (0.1 M) and 14.7 ml

HCl solution (0.1 M), and then diluted with DI water to 100 ml.

### 2.3 Design and preparation of microfluidic reactors

The two microfluidic reactors used in this work are schematically depicted in Fig. 1. The only difference of the structure of the two microfluidic reactors was the number of inlets for introducing reactant streams. There were two inlets for  $[\text{Cu}(\text{NH}_3)_4](\text{OH})_2$  and  $\text{N}_2\text{H}_4$  for the two-inlet design shown as inset A in Fig. 1a, while an additional inlet for introducing the buffer solution was added in for the three-inlet design shown as inset B in Fig. 1b. Due to the extremely low flow rates in the microfluidic reactors, normally on the magnitude of microliter per minute, the compressibility of aqueous solution and the flexibility of tubing connecting syringes and microfluidic reactors extended the time of the flow system required to get equilibrated significantly. A blind channel, “indicating channel” shown as inset C, was designed to monitor whether the flow system reached a stable state or not. The air spontaneously constrained in the “indicating channel” will be compressed after solutions were pumped into the microfluidic reactors. The motion of the air–liquid interface can be treated as a signal reflecting flow situations inside the microfluidic reactors. When the flowing solution

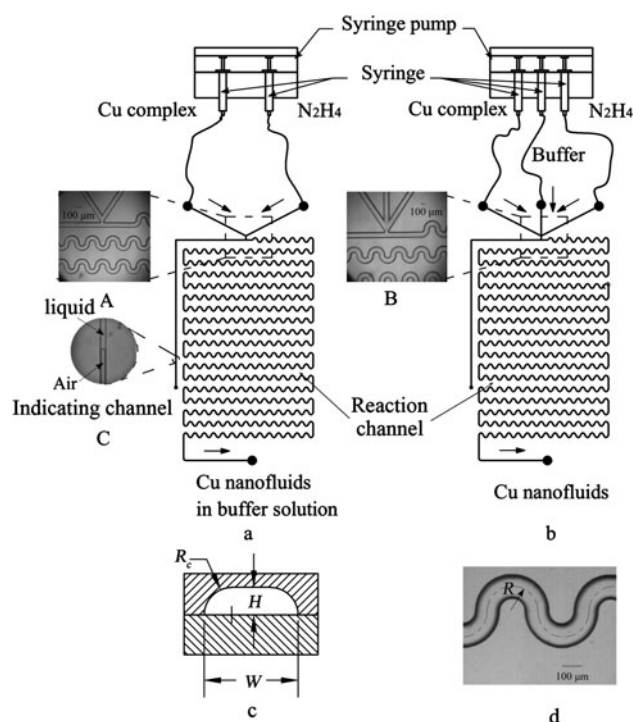


**Fig. 1** Schematics of microfluidic reactors: **a** two-inlet design, **b** three-inlet design, **c** cross-section of curved channel, and **d** micrograph of curved channel (*inset A* micrograph of two-inlet design, *inset B* micrograph of three-inlet design, *inset C* micrograph of air–liquid interface in the indicating channel)

reached a steady state, the interface had a fixed position corresponding to the total flow rate. The microfluidic reactors were fabricated in glass by using standard photolithographic technology (Tai-Ran 2002; Fang 2005; Ilescu et al. 2005; Chen et al. 2007; Tiggelaar et al. 2007). Commercial glass wafer was used, measuring  $60 \times 60 \text{ mm}^2$ , deposited with a 145 nm layer of chrome and a 570 nm layer of positive photoresist (SG2506, Shaoguang Chrome Blank Co., Ltd., China). The microchannels design, including both two-inlet and three-inlet design, printed on a film mask (Shenzhen New Way Electronics Co. Ltd., China) was transferred onto the photoresist layer after UV exposure in a UV exposure unit (LV204, Mega Electronics Ltd., UK). After development and chromium removing, the microchannels design was then etched on the glass wafer in a mixing solution of HF (1 M) and  $\text{NH}_4\text{F}$  (1 M) in an ultrasonic environment in room temperature (Cole-Parmer® 8893, Cole-Parmer Instrument Company, USA). The etched glass wafer was cut into two pieces to separate the two designs out. Another piece of polished glass tailored to the same sizes as the separated ones was used to seal the microchannels by thermal bonding in a programmable Muffle furnace after desiccation in a vacuum oven (Vulcan® 3-550, DENTSPLY Ceramco, USA; DZF-6020, Shanghai Shengxin Scientific Instrument Factory, China). Channel width was measured by using a vision-measuring machine, and channel depth was measured by using a surface roughness tester before thermal bonding (Quick Vision Pro 202; SV-3000S4, Mitutoyo Corporation, Japan). All channels etched in HF– $\text{NH}_4\text{F}$  solution had a bowl-shaped cross-section (Fig. 1c) resulted from the isotropic property of glass material in wet etching process. Geometrical characteristics of the cross-section of the winding reaction channels were as follows: longer width  $W = 121 \text{ }\mu\text{m}$ , depth  $H = 40 \text{ }\mu\text{m}$ , and side radius  $R_c = H$  resulted from wet etching. The cross-section area  $A$  and perimeter  $P$  of reaction channels can be calculated by Eqs. 1 and 2, respectively.

$$A = \frac{\pi R_c^2}{2} + (W - 2R_c)R_c \tag{1}$$

$$P = 2(W - R_c) + \pi R_c \tag{2}$$

The total length of the curved reaction channels was  $L = 2304 \text{ mm}$ , and the axial radius of curvature was  $R = 120 \text{ }\mu\text{m}$  as a constant as shown in Fig. 1d. So the volumetric capacity  $V_{\text{mr}}$  of the microfluidic reactors was  $9.5 \text{ }\mu\text{l}$  calculated from

$$V_{\text{mr}} = L \cdot A \tag{3}$$

In our experiments, chemical synthesis of copper nanofluids was normally found to be finished within 10-min scale by using traditional method in a 50 ml

boiling flask-3-neck. To ensure nanoparticles are fully synthesized in microfluidic reactors, a long reaction change is necessary for providing sufficient residence time. A curved reaction channel with a total length of more than 2 m was designed to do so. Another purpose of the utilization of long curved reaction channel is to introduce Dean vortices to provide an even efficient mixing for nanoparticles nucleation and growth. When a fluid flows through a curved channel, counter-rotating Dean vortices on the cross-section plane will arise from the interaction between viscous, inertial, and centrifugal forces (Jiang et al. 2004; Yamaguchi et al. 2004; Sudarsan and Ugaz 2006a, b; Ahn et al. 2008). The strength of Dean vortices is evaluated by Dean number, which is stated as:

$$Dn = Re \sqrt{\frac{D_h}{R}} \tag{4}$$

where  $Re$  is Reynolds number,  $D_h = 4A/P$  is the hydraulic diameter of reaction channels. Reynolds number indicates the relative ratio of inertial force to viscous force, and is stated as:

$$Re = \frac{\rho \bar{v} D_h}{\mu} \tag{5}$$

where  $\rho$  is fluid density,  $\mu$  is fluid viscosity, and  $\bar{v} = Q_{\text{total}}/A$  is the average velocity in reaction channels, where  $Q_{\text{total}}$  is the total volumetric flow rate in reaction channels. Here  $\rho$  and  $\mu$  should be the effective density and viscosity of copper nanofluids in reaction channels. In fact, we can safely and accurately use the density and viscosity of base fluid (DI water) in place of that of copper nanofluids in the application of Eqs. 4 and 5 due to the negligible influence of copper nanoparticles on the density and viscosity of base fluids at very low volume fraction of nanoparticles. The classic theoretical model to describe the effective viscosity of nanofluids with a low concentration of rigid spherical particles is developed by Einstein (Einstein 1956) and presented as:

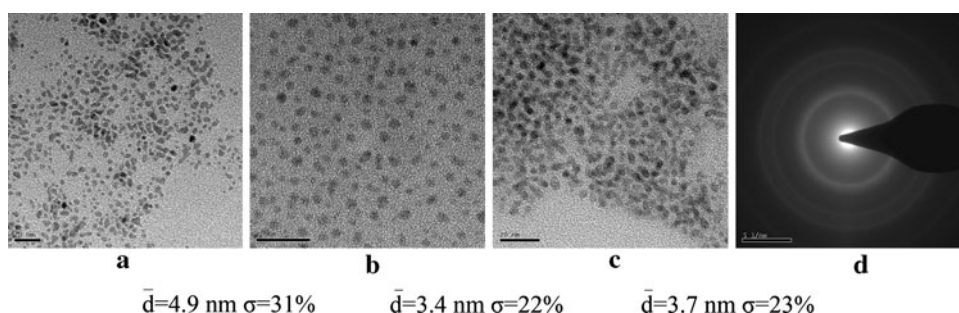
$$\mu_{\text{eff}} = \mu_{\text{bf}}(1 + 2.5\Phi) \tag{6}$$

where  $\mu_{\text{eff}}$  is the effective viscosity of nanofluids,  $\mu_{\text{bf}}$  is the viscosity of base fluids, and  $\Phi$  is the particle volume fraction. In our experiment, the highest molar concentration of copper hydroxide is 4 mM, and the resulted volume fraction of copper nanoparticles is extremely low, less than  $2.5 \times 10^{-4}$ . Therefore, the error of using base fluids density and viscosity to calculate  $Re$  and  $Dn$  is estimated to be less than 0.2%.

#### 2.4 Copper nanofluids synthesis by flask method

In a 50 ml boiling flask-3-neck, 20 ml diluted stock solution  $[\text{Cu}(\text{NH}_3)_4] \cdot (\text{OH})_2$  was added into 20 ml diluted  $\text{N}_2\text{H}_4$

**Fig. 2** TEM micrographs of copper nanoparticles synthesized by: **a** flask method, **b** two-inlet microfluidic reactor, **c** three-inlet microfluidic reactor, **d** SAED image of copper nanoparticles (4 mM  $[\text{Cu}(\text{NH}_3)_4]\cdot(\text{OH})_2$ , 120 mM  $\text{N}_2\text{H}_4$ , and 1 mM DBS)



solution containing surfactant DBS under a magnetic stirring at 400 round/min in room temperature. The mixed solution turned into light yellow immediately, implying a very fast reduction rate of  $\text{Cu}^{2+} \rightarrow \text{Cu}$ , and the color became denser gradually until no further color change after about 10 to 30 min stirring.

### 2.5 Copper nanofluids synthesis by microfluidic method

In the process of microfluidic synthesis, solutions were preloaded in 1 ml Gastight syringes (Gastight 1001, Hamilton Co., USA) to which microfluidic reactors were connected using Luer-Lock fittings and 1/16" PTFE tubing (Cole-Parmer, USA). The preloaded stock solutions were introduced into microfluidic reactors at the same volumetric flow rates propelled by a syringe pump (Cole-Parmer® 74900, Cole-Parmer Instrument Company, USA). The motion of the air–liquid interface in the “indicating channel” and the flow situation inside microfluidic reactors was monitored by an inversed microscope (XD101, Nanjing Jiangnan Novel Optics Co. Ltd., China) interfaced with a high-speed camera (MotionPro X4, IDT, Taiwan). Due to the ease of oxidization of copper nanoparticles, copper nanofluids were collected in the buffer solution to slow down the oxidization rate for the two-inlet design (Fig. 1a).

### 2.6 Nanoparticles characterization

Particle morphology, size, and size distribution were determined from image analysis of micrographs taken by a Transition Electron Microscope (Philips Tecnai G2 20 S-TWIN TEM microscope, FEI Co., USA), and the open software ImageJ was used to do so (Rasband WS, U.S. National Institutes of Health, Bethesda, Maryland, USA, 1997–2009). Observation of 150–300 particles for each sample was used in the calculation of average size (diameter),  $\bar{d}$ , and size distribution,  $\sigma$ , defined as the ratio of standard deviation to the average diameter. Measurement error in micrographs by using ImageJ was estimated to be less than 0.3 nm. To do TEM measurement, samples were

first dripped onto a 400-mesh carbon-coated copper grid (G400 Square Mesh, SPI supplies, USA), followed by washing with absolute alcohol, and then dried at ambient atmosphere. Typical micrographs of copper nanoparticles synthesized in either the flask or the microfluidic reactors were shown in Fig. 2a–c. Element of the nanoparticles was confirmed by doing selected area electron diffraction (SAED) measurement on 400-mesh carbon-coated nickel grids (G400 Square Mesh, SPI supplies, USA). By comparing the lattice spacing based on rings in the SAED micrograph (Fig. 2d) with the standard atomic spacing along their characteristic *hkl* index documented in the powder diffraction file (PDF), the nanoparticles synthesized by chemical method in this study were verified as copper nanocrystal.

## 3 Results and discussion

### 3.1 Influence of flow rates on particle size

During the experiment, it was found that the syringe pump could not operate at very high flow rates. When the total flow rate was over 30  $\mu\text{l}/\text{min}$ , the syringe pump would be stalled because the frictional resistance inside the microfluidic reactor was too large to be overcome by syringe pump thrust. In another hand, flow rates cannot be too low. One had to wait at least 10 min, some time several hours, to let the flow system reach a steady state after every change of flow rate, judging from the air–liquid interface motion in the “indicating channel” (inset C in Fig. 1). The lower the flow rates were, the longer the time needed. If the flow rates were too low, the waiting time could be extremely long and sometimes even no nanoparticles could be detected in the nanofluids that just flowed out the microfluidic reactors, for instance, when the total flow rate was around 0.2  $\mu\text{l}/\text{min}$  for the two-inlet design.

To investigate the influence of flow rate on nanoparticle size and size distribution, we synchronously changed both flow rates of the two stock solutions from 1.25 to 10  $\mu\text{l}/\text{min}$ , resulting in a total flow rate variation from 2.5 to 20  $\mu\text{l}/\text{min}$  in Fig. 1a. Hereafter without especial specification the



microfluidic reactor used to investigate the influence of flow rates, reactants concentrations, and DBS concentrations was the one with two inlets configuration (Fig. 1a). The concentration of  $[\text{Cu}(\text{NH}_3)_4] \cdot (\text{OH})_2$  solution was set at 4 mM, and the reducing solution  $\text{N}_2\text{H}_4$  containing 1 mM DBS was retained at 120 mM. The average residence time  $\bar{t}_r$  of the two precursors in the microfluidic reactor is directly related to the total flow rate, which is stated as:

$$\bar{t}_r = \frac{V_{\text{mr}}}{Q_{\text{total}}} \quad (7)$$

As the total flow rate increases from 2.5 to 20  $\mu\text{L}/\text{min}$ , the average residence time decreases from 227 to 28 s. Since the average residence time when  $Q_{\text{total}} = 20 \mu\text{L}/\text{min}$  is much smaller than the synthesis time observed in flask manner, nanoparticle synthesis might still be in progress in the receiving container if it was not fully conducted inside the microfluidic reactor. To testify, the copper nanoparticles were fully synthesized in the microfluidic reactor in that case, we made a comparison of the samples taken from the collecting container and that collected just flowed out the outlet. It was found that the particle size and size distribution were almost the same, and no distinct difference was detected. More over, the comparison revealed that by using the microfluidic reactor the synthesis time of copper nanoparticles was drastically decreased as much as one order of magnitude, compared with traditional flask method that usually took 10–30 min to fully finish the synthesis.

Figure 3 depicts that the total flow rate has little impact on particle size when it is changed from 2.5 to 20  $\mu\text{L}/\text{min}$ . The average size is around 3.3 nm, and the coefficient of variation is about 22% for all the samples collected at different flow rates. The insensitivity of particle size and

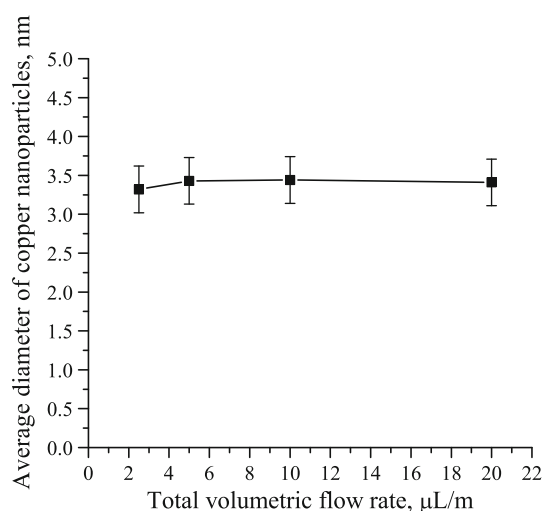


**Fig. 3** Dependence of the average particle size on the total volumetric flow rate, generated in the two-inlet design (4 mM  $[\text{Cu}(\text{NH}_3)_4] \cdot (\text{OH})_2$ , 120 mM  $\text{N}_2\text{H}_4$ , and 1 mM DBS)

size distribution to the flow rates may be explained by the same mixing mechanism for copper nucleation in the reaction channel. In the range of flow rates studied, mixing for copper nucleation in the microfluidic reactor is mainly dominated by mass diffusion because of the extremely low  $Re$  and  $Dn$ , where the Dean vortices are not strong enough to induce intensive transverse convection and then cause a discrepancy in mixing efficiency at different flow rates. Numerical studies of mixing in curved square/circular ducts at low  $Re$  have shown that for fluids with large Schmidt number ( $\mu/\rho D = 1000$ , where  $D$  is mass diffusivity), mixing is hardly influenced by Dean vortices when  $Re$  is of order of unity, and the mixing is primarily diffusion driven (Kumar et al. 2006). A detailed comparison between numerical and experimental investigation of fluid mixing in a 200  $\mu\text{m}$  square curved channel has also revealed that for low Dean number ( $\sim 10$ ) no chaotic mixing occurs, and the inter-diffusion area approximately moves back to its original position when channel curvature is reversed (Yamaguchi et al. 2004). In this work, as the total flow rate increases from 2.5 to 20  $\mu\text{L}/\text{min}$ ,  $Re$  increases from 0.6 to 4.7 and  $Dn$  number increases from 0.4 to 3.2. Either  $Re$  or  $Dn$  is below the threshold ( $Re \sim 5$  or  $Dn \sim 10$ ) at which Dean vortices will significantly enhance the mixing in microchannels. In common with other colloidal formation by chemical synthesis, copper nanoparticles are formed starting from an initial homogeneous nucleation in which tiny nuclei precipitate spontaneously from solutions and a subsequent growth phase in which the freshly formed nuclei capture dissolved atoms or molecules by diffusion (LaMer and Dinigar 1950; Hosokawa et al. 2007). Particle size and size distribution are strongly influenced by the quality of nuclei formed in the nucleation phase which is significantly influenced by the mixing efficiency of precursors. In intermixing area between the two reactant streams, large amount of copper atoms appears because of the high reduction rate, and then a quick nucleation process arise. After fully mixed, the similar number of copper nuclei forms at different flow rates due to the same mixing mechanism—mass diffusion. The formed copper nuclei absorb copper atoms generated from chemical reaction to further increase particle size until all copper atoms are consumed. Therefore, the copper nanoparticles finally grow up to a similar size regardless of the flow rates.

### 3.2 Influence of reactants concentrations

The influence of reactants concentrations on particle size has been investigated, in both microfluidic reactor way and flask way, by altering the concentrations of  $[\text{Cu}(\text{NH}_3)_4] \cdot (\text{OH})_2$  from 0.5 to 8 mM while keeping a fixed concentration ratio at 4:120:1 for  $[\text{Cu}(\text{NH}_3)_4] \cdot (\text{OH})_2:\text{N}_2\text{H}_4:\text{DBS}$ . Figure 4

shows that reactants concentrations have little influence on copper nanoparticles synthesized in the microfluidic reactor. The average particle size is around 3.4 nm, and the variation of coefficient is about 22%. The insensitivity of particle size and size distribution to the reactants concentration may be interpreted as a result of the very fast and efficient mass diffusion of reactants in the microfluidic reactor. The mixing time by which fully mixed precursors can be obtained is estimated as:

$$t_d \sim \frac{(W/2)^2}{D} \quad (8)$$

where  $D$  is the mass diffusivity of  $\text{Cu}/\text{N}_2\text{H}_4$  in water. Given  $D$  is on the order of  $10^{-9} \text{ m}^2/\text{s}$ ,  $t_d$  is estimated around only 3.6 s. With the help of fast and efficient mixing, copper atoms have an equal opportunity to aggregate to form copper nuclei. At a higher concentration, larger amount copper nuclei will arise from once or multiple nucleation, and much more copper atoms are consumed in the nucleation phase; while at a lower concentration, less amount copper nuclei will be formed, and less copper atoms are consumed. Therefore, at the end of growth phase copper nanoparticles synthesized in the microfluidic reactor at either high or low reactants concentrations will have a similar average size and size distribution. However, in flask method copper nanoparticle size exhibits an unpredictable dependence on reactants concentrations, which could be resulted from the uncontrollable balance between mixing efficiency, reactants concentrations and copper nucleation rate according to the classical nucleation mechanism. The average particle size varies from 2.7 to 4.9 nm with a broad size distribution, larger than 30%, as shown in Fig. 4.

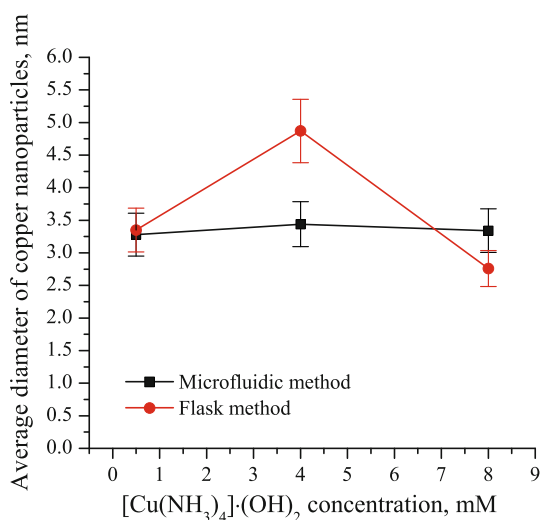


**Fig. 4** Dependence of the average nanoparticle size on the concentration of copper complex, generated in the two-inlet design. ( $C([\text{Cu}(\text{NH}_3)_4] \cdot (\text{OH})_2) : C(\text{N}_2\text{H}_4) : C(\text{DBS}) = 4 : 120 : 1$ )

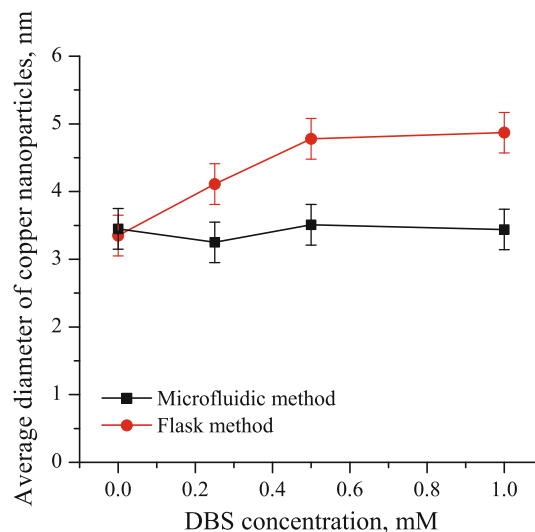


**Fig. 5** Dependence of the average nanoparticle size on the concentration of surfactant DBS, generated in the two-inlet design. ( $C([\text{Cu}(\text{NH}_3)_4] \cdot (\text{OH})_2) = 4 \text{ mM}$ ,  $C(\text{N}_2\text{H}_4) = 120 \text{ mM}$ )

### 3.3 Influence of DBS concentration

The influence of DBS at different concentrations on particle size synthesized in the microfluidic reactor as well as in the flask has been investigated. The concentration of DBS in  $\text{N}_2\text{H}_4$  solution was changed from 0 to 1 mM while keeping the concentration of  $[\text{Cu}(\text{NH}_3)_4] \cdot (\text{OH})_2$  and  $\text{N}_2\text{H}_4$  at 4 and 120 mM, respectively. It is found that, shown in Fig. 5, the concentration of DBS has little influence on nanoparticle size synthesized in the microfluidic reactor; and the average particle size is around 3.4 nm with a variation of coefficient of about 23%. However, the average size of particles synthesized in the flask increases from 3.3 to 4.9 nm as DBS concentration increases, and the size distribution is usually larger than 30%. The large discrepancy of the influence of DBS on particle size is probably resulted from the different mixing mechanism for copper nucleation and growth for these two methods. In the microfluidic reactor, mixing for nucleation is mainly dominated by mass diffusion, while in the flask mixing is mainly dominated by convection. In the limit of low  $Re$ , for spherical particles, the Einstein relation describing the diffusivity of particles is expressed as:

$$D = \frac{K_B T}{6\pi\mu r} \quad (9)$$

where  $K_B$  is the Boltzmann constant,  $T$  is the absolute temperature, and  $r$  is the diameter of particles including molecules or atoms. For a copper atom the diameter is on the order of  $10^{-10} \text{ m}$ , and the diffusivity is on the order of  $10^{-9} \text{ m}^2/\text{s}$  in water, based on Eq. 9. In aqueous solutions, surfactant DBS ( $\text{C}_{18}\text{H}_{29}\text{SO}_3\text{Na}$ ) dissociates a long chain group with surface activity  $\text{C}_{18}\text{H}_{29}\text{SO}_3^-$  of which the

equivalent diameter is at least one order higher than that of a copper atom. According to Eq. 9, the diffusivity of  $C_{18}H_{29}SO_3^-$  is on the order of  $10^{-10} \text{ m}^2/\text{s}$  that is one order smaller than that of a copper atom. The higher the diffusivity is, the faster the particles transport in liquid by diffusion. Copper atoms aggregate to form nuclei and are further absorbed onto formed nuclei at a much higher speed than the adsorption of  $C_{18}H_{29}SO_3^-$ . The large discrepancy of diffusivity weakens the influence of DBS on the size of copper nanoparticles synthesized in the microfluidic reactor. In flask method, precursors are under a strong stirring where the mixing is dominated by fluid convection. The intensive fluid convection will promote the motion of both  $C_{18}H_{29}SO_3^-$  and copper atoms, and relatively reduce the difference of aggregation rate between copper atoms and DBS such that the influence of DBS on particle size is visible.

### 3.4 Stability improvement of copper nanofluids

Copper nanofluids synthesized by chemical reduction without pH adjustment are found to have a poor stability due to the oxidization of copper nanoparticles, and the freshly synthesized copper nanofluids can only stand for  $\sim 2$  h without obvious oxidization or precipitation in open air in room temperature. In our previous study, it was found that pH adjustment of copper nanofluids would effectively slow down the oxidization rate and the effective pH range was located between 8.45 and 8.65 (Jiang and Wang 2009). Therefore, a Tris–HCl buffer solution with a pH = 8.5 was used to collect copper nanofluids, which usually took several hours to get enough samples. After pH adjustment, the copper nanofluids can normally stand for 5 h including the time consumed in the collection process without obvious oxidization or precipitation. The three-inlet microfluidic reactor (Fig. 1b) was designed to do so by introducing the buffer solution between  $[Cu(NH_3)_4] \cdot (OH)_2$  and  $N_2H_4$  during chemical reaction rather than after reaction finished. It is found in such a flow configuration the copper nanofluids have a similar stability as that synthesized without but collected in the buffer solution.

### 3.5 Aggregation of nanoparticles on channel walls

Copper nanoparticle agglomeration on channel surfaces was found in our experiments in either two- or three-inlet design. Figure 6 shows a typical agglomeration of copper nanoparticles on microchannel walls. At present time it seems that effective methods to prevent nanoparticles from aggregating on channel walls are still unavailable for such continuous synthesis in microfluidic reactors. Particle agglomeration on channel surfaces is affected by many parameters among which the running time and the reactants

concentrations are found to be the most important ones. Severe aggregation normally appears after a long time running of chemical reaction at a high concentration. For 4 mM  $[Cu(NH_3)_4] \cdot (OH)_2$ , agglomeration of copper nanoparticles would be found after  $\sim 3$  h running at a total flow rate of  $10 \mu\text{l}/\text{min}$  (Fig. 6a), and severe agglomeration is found after  $\sim 5$  h running (Fig. 6b). The agglomeration situation after introducing buffer solution, running at a total flow rate of  $10 \mu\text{l}/\text{m}$  for 4 h, is shown in Fig. 6c.

## 4 Concluding remarks

Synthesis of copper nanofluids has been realized in microfluidic reactors. Although agglomeration of nanoparticles on channel walls is still a challenge, a variety of benefits arising from the fast and efficient mixing have been demonstrated, including the insensitivity of nanoparticle size and size distribution to flow rates of reactants, reactants concentrations, and surfactant concentrations. In comparison to flask method, copper nanofluids containing nanoparticles with a uniform size distribution can be achieved by using microfluidic reactors. Copper nanoparticles synthesized by microfluidic reactors have an average size around 3.4 nm with a coefficient of variation of about 22%, whereas the average size of copper nanoparticles synthesized by flask method changes from 2.7 to 4.9 nm with a coefficient of variation larger than 30%, depending on the concentrations of  $[Cu(NH_3)_4] \cdot (OH)_2$  and DBS. Moreover, by using microfluidic reactors, the synthesis time of copper nanofluids is reduced one order of magnitude, from  $\sim 10$  min to  $\sim 28$  s. Dean vortices effectively used in micromixing technology have limited applications on enhancing the mixing efficiency for nanofluid synthesis because of the extremely low  $Re$  and  $Dn$ , normally on the order of unity. Unlike pure micromixers, microfluidic reactors must have such a feature that to provide long enough residence time for nanoparticles nucleation and growth. That can probably be realized by slowing down flow velocity in the reaction channel or by increasing the length of reaction channel. However, low flow velocity directly causes low  $Re$  and  $Dn$  and negligible transverse

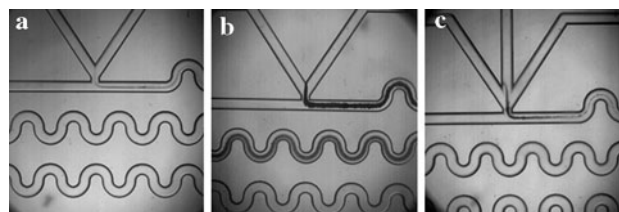


**Fig. 6** Aggregation of copper nanoparticles on channel walls, flowing at a total flow rate of  $10 \mu\text{l}/\text{min}$  after: **a** 3 h, **b** 5 h, **c** 4 h (4 mM  $[Cu(NH_3)_4] \cdot (OH)_2$ , 120 mM  $N_2H_4$ , and 1 mM DBS)

convection, and long reaction channel will result in operational difficulties on the high flow resistance and the manufacture of microfluidic reactors.

**Acknowledgments** The financial support from the Research Grants Council of Hong Kong (GRF718009) is gratefully acknowledged. The authors would also like to thank Mr. Frankie Y. F. Chan at Electron Microscope Unit, HKU, for his support in taking TEM images.

## References

- Ahn YC, Jung WG, Chen ZP (2008) Optical sectioning for microfluidics: secondary flow and mixing in a meandering microchannel. *Lab Chip* 8(1):125–133
- Cashion LM, Bare LA, Harvey S, Trinh Q, Zhu Y, Devlin JJ (1999) Use of enhanced green fluorescent protein to optimize and quantitate infection of target cells with recombinant retroviruses. *Biotechniques* 26(5):924
- Chan EM, Mathies RA, Alivisatos AP (2003) Size-controlled growth of CdSe nanocrystals in microfluidic reactors. *Nano Lett* 3(2):199–201
- Chan EM, Alivisatos AP, Mathies RA (2005) High-temperature microfluidic synthesis of CdSe nanocrystals in nanoliter droplets. *J Am Chem Soc* 127(40):13854–13861
- Chang H, Tsung TT, Chen LC, Yang YC, Lin HM, Han LL, Lin CK (2004) TiO<sub>2</sub> nanoparticle suspension preparation using ultrasonic vibration-assisted arc-submerged nanoparticle synthesis system (ASNSS). *Mater Trans* 45(3):806–811
- Chen DH, Liao MH (2002) Preparation and characterization of YADH-bound magnetic nanoparticles. *J Mol Catal B* 16(5–6):283–291
- Chen Q, Li G, Jin QH, Zhao JL, Ren QS, Xu YS (2007) A rapid and low-cost procedure for fabrication of glass microfluidic devices. *J Microelectromech Syst* 16(5):1193–1200
- Choi SUS (1995) Enhancing thermal conductivity of fluids with nanoparticles. In: Proceedings of the 1995 ASME international mechanical engineering congress and exposition San Francisco, CA, USA
- Das SK, Choi SUS, Patel HE (2006) Heat transfer in nanofluids—a review. *Heat Transf Eng* 27(10):3–19
- Edel JB, Fortt R, deMello JC, deMello AJ (2002) Microfluidic routes to the controlled production of nanoparticles. *Chem Commun* (10):1136–1137
- Einstein A (1956) Investigations on the theory of the Brownian movement. Dover Publications, Inc., New York
- Fang Z (2005) Manufacture and applications of microfluidic chips. Chemical Industry Press, Beijing
- Hosokawa M, Nogi K, Naito M, Yokoyama T (2007) Nanoparticle technology handbook. Elsevier, Amsterdam
- Iliescu C, Tay FE, Ieee (2005). Wet etching of glass. International semiconductor conference, Sinaia, Romania
- Jackman RJ, Floyd TM, Ghodssi R, Schmidt MA, Jensen KF (2001) Microfluidic systems with on-line UV detection fabricated in photodefinable epoxy. *J Micromech Microeng* 11(3):263–269
- Jiang W, Wang LQ (2009) Copper nanofluids: synthesis and thermal conductivity (submitted)
- Jiang F, Drese KS, Hardt S, Kupper M, Schonfeld F (2004) Helical flows and chaotic mixing in curved micro channels. *AIChE J* 50(9):2297–2305
- Karnik R, Gu F, Basto P, Cannizzaro C, Dean L, Kyei-Manu W, Langer R, Farokhzad OC (2008) Microfluidic platform for controlled synthesis of polymeric nanoparticles. *Nano Lett* 8(9):2906–2912
- Kohler JM, Abahmane L, Wagner J, Albert J, Mayer G (2008) Preparation of metal nanoparticles with varied composition for catalytical applications in microreactors. *Chem Eng Sci* 63(20):5048–5055
- Krishnadasan S, Tovilla J, Vilar R, deMello AJ, deMello JC (2004) On-line analysis of CdSe nanoparticle formation in a continuous flow chip-based microreactor. *J Mater Chem* 14(17):2655–2660
- Kumar V, Aggarwal M, Nigam KDP (2006) Mixing in curved tubes. *Chem Eng Sci* 61(17):5742–5753
- LaMer VK, Dinegar RH (1950) Theory, production and mechanism of formation of monodispersed hydrosols. *J Am Chem Soc* 72(11):4847–4854
- Laulicht B, Cheifetz P, Mathiowitz E, Tripathi A (2008) Evaluation of continuous flow nanosphere formation by controlled microfluidic transport. *Langmuir* 24(17):9717–9726
- Lee S, Choi SUS, Li S, Eastman JA (1999) Measuring thermal conductivity of fluids containing oxide nanoparticles. *J Heat Transf Trans ASME* 121(2):280–289
- Liu MS, Lin MCC, Tsai CY, Wang CC (2006) Enhancement of thermal conductivity with Cu for nanofluids using chemical reduction method. *Int J Heat Mass Transf* 49(17–18):3028–3033
- Lo CH, Tsung TT, Chen LC (2005a) Shape-controlled synthesis of Cu-based nanofluid using submerged arc nanoparticle synthesis system (SANSS). *J Cryst Growth* 277(1–4):636–642
- Lo CH, Tsung TT, Lin HM (2005b) Preparation of silver nanofluid by the submerged arc nanoparticle synthesis system (SANSS). In: 12th international symposium on metastable and nano-materials (ISMANAM-2005), Paris, France
- Shalom D, Wootton RCR, Winkle RF, Cottam BF, Vilar R, deMello AJ, Wilde CP (2007) Synthesis of thiol functionalized gold nanoparticles using a continuous flow microfluidic reactor. *Mater Lett* 61(4–5):1146–1150
- Shestopalov I, Tice JD, Ismagilov RF (2004) Multi-step synthesis of nanoparticles performed on millisecond time scale in a microfluidic droplet-based system. *Lab Chip* 4(4):316–321
- Song YJ, Kumar C, Hormes J (2004) Synthesis of palladium nanoparticles using a continuous flow polymeric micro reactor. *J Nanosci Nanotechnol* 4(7):788–793
- Song YJ, Doomes EE, Prindle J, Tittsworth R, Hormes J, Kumar C (2005) Investigations into sulfobetaine-stabilized Cu nanoparticle formation: Toward development of a microfluidic synthesis. *J Phys Chem B* 109(19):9330–9338
- Song YJ, Modrow H, Henry LL, Saw CK, Doomes EE, Palshin V, Hormes J, Kumar C (2006) Microfluidic synthesis of cobalt nanoparticles. *Chem Mater* 18(12):2817–2827
- Sudarsan AP, Ugaz VM (2006a) Fluid mixing in planar spiral microchannels. *Lab Chip* 6(1):74–82
- Sudarsan AP, Ugaz VM (2006b) Multivortex micromixing. *Proc Natl Acad Sci USA* 103(19):7228–7233
- Tai-Ran H (2002) MEMS & Microsystems design and manufacture. McGraw-Hill, New York
- Tiggelaar RM, Benito-Lopez F, Hermes DC, Rathgen H, Egberink RJM, Mugele FG, Reinhoudt DN, van den Berg A, Verboom W, Gardeniers H (2007) Fabrication, mechanical testing and application of high-pressure glass microreactor chips. *Chem Eng J* 131(1–3):163–170
- Trisaksri V, Wongwises S (2007) Critical review of heat transfer characteristics of nanofluids. *Renew Sustain Energy Rev* 11(3):512–523
- Wagner J, Kohler JM (2005) Continuous synthesis of gold nanoparticles in a microreactor. *Nano Lett* 5(4):685–691
- Wagner J, Kirner T, Mayer G, Albert J, Kohler JM (2003) Generation of metal nanoparticles in a microchannel reactor. In: 7th international conference on microreaction technology (IMRET 7), Lausanne, Switzerland



- Wang XQ, Mujumdar AS (2008) A review on nanofluids—Part II: experiments and applications. *Braz J Chem Eng* 25(4):631–648
- Wang LQ, Wei XH (2009) Heat conduction in nanofluids. *Chaos Solitons Fractals* 39(5):2211–2215
- Wang HZ, Nakamura H, Uehara M, Miyazaki M, Maeda H (2002) Preparation of titania particles utilizing the insoluble phase interface in a microchannel reactor. *Chemical Commun* (14):1462–1463
- Wang HZ, Li XY, Uehara M, Yamaguchi Y, Nakamura H, Miyazaki MP, Shimizu H, Maeda H (2004) Continuous synthesis of CdSe–ZnS composite nanoparticles in a microfluidic reactor. *Chem Commun* (1):48–49
- Wei XH, Zhu HT, Wang LQ (2009) CePO<sub>4</sub> nanofluids: synthesis and thermal conductivity. *J Thermophy Heat Transf* 23(1):219–222
- Wen DS, Lin GP, Vafaei S, Zhang K (2009) Review of nanofluids for heat transfer applications. *Particuology* 7(2):141–150
- Xuan YM, Li Q (2000) Heat transfer enhancement of nanofluids. *Int J Heat Fluid Flow* 21(1):58–64
- Xue ZL, Terepka AD, Hong Y (2004) Synthesis of silver nanoparticles in a continuous flow tubular microreactor. *Nano Lett* 4(11):2227–2232
- Yamaguchi Y, Takagi F, Watari T, Yamashita K, Nakamura H, Shimizu H, Maeda H (2004) Interface configuration of the two layered laminar flow in a curved microchannel. *Chem Eng J* 101(1–3):367–372
- Yatsuya S, Hayashi T, Akoh H, Nakamura E, Tasaki A (1978) Magnetic-properties of extremely fine particles of iron prepared by vacuum evaporation on running oil substrate. *Jpn J Appl Phys* 17(2):355–359
- Yatsuya S, Tsukasaki Y, Yamauchi K, Mihama K (1984) Ultrafine particles produced by vacuum evaporation onto a running oil substrate (VEROS) and the modified method. *J Cryst Growth* 70(1–2):533–535
- Zhu HT, Lin YS, Yin YS (2004) A novel one-step chemical method for preparation of copper nanofluids. *J Colloid Interface Sci* 277(1):100–103